IJE TRANSACTIONS B: Application Vol. 26, No. 8, (August 2013) 885-894

International Journal of Engineering

Journal Homepage: www.ije.ir

Mixed Mode Crack Propagation of Zirconia/Nickel Functionally Graded Materials

A. R. EL-Desouky, M. S. EL-Wazery*

Department of Production Engineering and Mechanical Design, Faculty of Engineering, Menoufiya University, Shebin El-Kom, Egypt

PAPER INFO

Paper history:
Received 08 February 2013
Received in revised form 23 May 2013
Accepted 20 June 2013

Keywords:
Functionally Graded Materials (FGM)
Powder Metallurgy Technique
Mixed Mode Fracture
Finite Element Method
Non-graded Composite (NGCS)
Maximum Principle Stress (MPS)

ABSTRACT

Zirconia-nickel functionally graded materials were obtained by powder metallurgy technique. The microstructure, residual stress, fracture toughness and Vickers hardness were investigated. Mixed-mode fracture response of YSZ /Ni functionally graded materials was examined utilizing the three point bending test and finite element method (Cosmos/M 2.7). The results show that the stress intensity factors (K_I, K_{II}) for the FGM are less than those for non-graded composite (NGCs) under mixed mode loading conditions. There are some local perturbations in the crack propagation paths of the FGM and NGC specimens. Most of local perturbations exhibit in the layers with high Ni content such as the layers with 30%, 40% and 50% Ni, respectively. The local perturbations are believed to be caused by the local heterogeneity of the microstructure. The residual stress (maximum tensile stress) of the NGC (YSZ/50%Ni) was 122 MPa and was in agreement with the published paper.

doi: *10.5829/idosi.ije.2013.26.08b.10*

1. INTRODUCTION

Functionally graded materials (FGMs) are innovative composite materials characterized by a gradual spatial change in composition, microstructure and related properties. FGMs are ideal candidates for the applications requiring multifunctional performance. For example, the ceramic/metal FGMs can be designed to reduce thermal stresses and take advantage of the heat and corrosion resistances of ceramic and the mechanical strength of metal. Due to the variation of properties, the fracture behavior in FGMs is very complicated [1-5].

Mixed mode crack growth is due to superposition of two or three loading modes: I-Tension, II-Shear, and III-Torsion. Most experiential fracture researches have been concerned with mode I loading since this is the most common mode for crack growth. However, initiation and growth of cracks, in practical situations can be mixed mode. In the practical situations, mode II and mode III loadings usually do not lead to fracture. Hence, the determination of the stress intensity factors for mixed mode in the cracked FGMs materials is the most practical problems in engineering [6-10]. The maximum Principle stress criterion is one of the realist theories dealing with stable mixed mode crack growth direction under static loading. According to this theory, the crack propagates in a direction normal to the maximum tangential stress. Jin et al. [11] have investigated the mixed-mode fracture response of ZrO_2/NiCr functionally graded materials (FGMs) using fracture test, digital image correlation technique and extended finite element method. The crack in the non-FGM specimen shows a continuous growth along a straight line except for a little perturbation. When the crack propagates along the direction of increasing fracture toughness, the specimen exhibits an enhanced R curve behavior. Kim and Paulino [12] studied the fracture behavior of FGMs under mechanical loading by performing automatic simulation of the crack propagation FGM through remeshing algorithm in conjunction with the finite element method. Crack trajectories obtained by fracture criterion agree well with available experimental results for homogenous and FGMs [13].

In this article, a detailed experimental investigation was conducted to study the influences of the varied mechanical properties (fracture toughness K_{IC}) on the fracture response of YSZ /Ni FGMs under the mixed-mode loading condition. The FGMs consisting of YSZ and Ni was fabricated by powder metallurgy. The

* Corresponding Author Email: sissy311945@yahoo.com (M. S. EL-Wazery)

distribution curve of K_{IC} in the YSZ /Ni FGMs was obtained from the tests conducted on the homogeneous specimens with different volume fractions of Ni. The mixed-mode loadings were generated by offsetting the crack notch relative to the loading point. The influences of the gradients of fracture toughness on the crack propagation were analyzed. In addition, according to the maximum hoop stress criterion, the crack propagation was predicted by MPS criteria and finite element method (Cosmos/M 2.70), respectively.

2. MATERIALS AND EXPERIMENTAL PROCEDURE

2. 1. Processing and Materials Yttria stabilized zirconia (3 mol % Y_2O_3) powder and Ni powder were used as the raw powders to fabricate the FGMs by utilizing the powder metallurgy technique. Zirconia (TZ-3Y) was used to form pure ceramic layer while nickel average particle size was 10 μm (MERK /USA), The mean particle sizes of powders were 0.3 μm for the YSZ (TOSOH, Japan) and 10 μm for the Ni, respectively. The chemical composition of Ni are listed in Table 1. The YSZ and Ni powders were mixed in volume ratios of 10–0, 9–1, 8-2, 7–3, 6-4 and 5–5, respectively. Mixing was done by wet milling in small plastic bottles with agate zirconia balls using a horizontal ball miller in ethanol. The number of the plastic bottles was six bottles according to model structures and each mixture was suspended in ethanol, milled for five hrs by utilizing the horizontal ball miller. The ratio of powder to ball was 1:2 and the milling speed was 100 r.p.m. Then, 30wt. % ethanol was added to the mixtures powders to cover the media (balls).

After milling, the mixed powders were sieved using a 250 μm steel mesh to remove the remaining agglomerates. 10wt. % Ethel alcohol binder was added to the powders which were used for forming pure ceramic and intermediated layers to lubricate particle contact. Then, the mixture powders were dried in a furnace at 70 ºC for 24 hrs. The powder blends were put to form a non-graded composition or were layered so as to form graded composition in a rectangular hot work tool steel die with 35 mm length and 10 mm width. The powder compacts were pressed up to (0.1 MPa) at room temperature for one minute. The powder compacts were pressed up to 0.5 MPa at room temperature for one minute. Hydraulic press machine was used to compact the powder layers once at the same pressure. After the pressing, the powder compacts were exited by the pressing. The die and punch set-up used to produce the non-graded composites and functionally graded materials (FGM) are reviewed in our papers [14, 15]. Using the same pressing conditions, a larger thickness (6.5 mm) FGM green compact was also formed but under lower pressure during stacking the layers, which would be used for mechanical property testing.

TABLE 1. Chemical Composition of Ni

Ni (wt. %)					
Fe	**O_2**	**Na**	**C**	**Co**	**Ni**
0.002	0.12	0.0125	0.1	0.0001	Balance

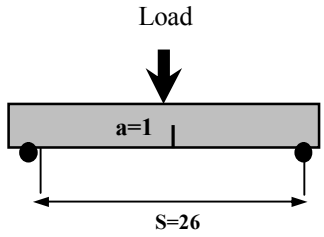

Figure 1. Schematics of the fracture test Dim in mm

The formed FGM and NGC compacts were subjected to pressureless sintering inside a tube furnace under vacuum at 1400 ◦C for 2 hour to prevent oxidation. The heating rate was 18 ◦C/min up to 1400 ◦C. The vacuum pressure of sintering furnace was 10^{-4} mbar. The inert gas (argon) was used to clean the furnace before the sintering process. Then, all compacts were furnace cooled to minimize residual stresses.

2. 2. Mechanical Testing The variations of fracture toughness (K_{IC}) in the FGMs were investigated directly from the three point-bending tests (3PBT) as shown in (Figure 1) on the homogenous NGC specimens. Fracture tests were conducted on Lloyd LR 10kN universal testing machine at crosshead speed of 0.1 mm/min.

According the fracture test, an edge crack with the length 1 mm, the width 0.3 mm and the root radius 0.150 mm is cut along the mid-span of the fracture specimen utilizing high speed diamond circular saw. Fracture toughness K_{IC} is calculated by the

$$K_{IC} = \frac{3PSY\sqrt{a}}{2WB} \quad (1)$$

where, P, S, a, W and B are the fracture load, span length, crack size, specimen width and specimen thickness, respectively. Y is a correction factor of the stress intensity factor and given as a function of a/w= 0.33 [13]. The average fracture toughness for each material composition was taken from three pieces test.

2. 3. Mixed Mode Fracture Test To exclude the influences of specimen geometry and loading condition on the fracture behavior, all specimens with an identical geometry were prepared. The FGM specimens were tested under the mixed-mode loading condition by initial notch at an offset distance (δ = 3 mm) from the loading line, as shown in Figure 2.

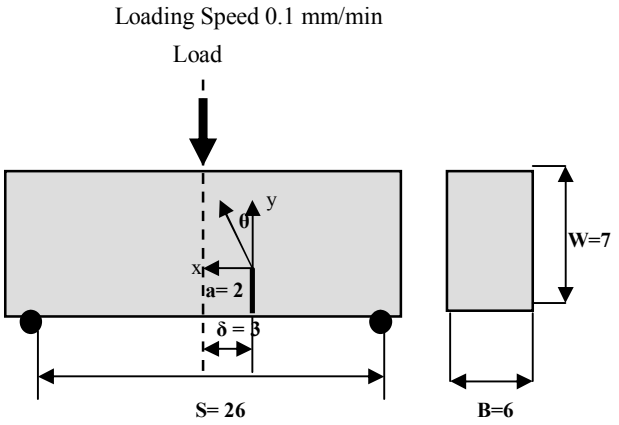

Figure 2. Schematics of the mixed mode fracture test.

An edge notch (root radius ≈0.150 mm and length 2 ± 0.01 mm) was cut along the mid-span of each FGM specimen through the pure ceramic (YSZ) face and the composite layer (50% Ni/ YSZ) face. For the FGM specimens, the edge notch was parallel to the material gradient. The mixed-mode fracture test was conducted on the Lloyd LR 10K universal testing machine at the crosshead speed of 0.1 mm/min.Crack behavior in YSZ /Ni FGMs and NGC (50%Ni/ YSZ) under mixed mode loading have been theoretically studied according to the fracture mechanics criterion such that; the stress intensity factors (SIFs). The SIFs of mode I and mode II can be determined from the following relations [16]:

$$K_I = \frac{3PS\sqrt{\pi .a}}{B.W^2} F_I\left(\frac{a}{w}\right) \quad (1)$$

$$K_{II} = \frac{3P\sqrt{\pi .a}}{2B.W} F_{II}\left(\frac{a}{w}\right) \quad (2)$$

where, K_I and K_{II} are the stress intensity factors of mode I, mode II, respectively, F_I (a/w) and F_{II} (a/w) are the corresponding correlation factors that depend on loading mode, and geometry**.** The ratio between a and w was 0.28, where a_0 is the initial notch length, w is the thickness, and B is the width of the specimen. The applied load was effected vertically at the center of the specimen, while the notch line was offset distance (δ= 3 mm) from the initial center line (center of symmetric). The crack geometry factors (correction factors) F_I and F_{II} can be estimated as follows [16].

$$F_I\left(\frac{a}{w}\right)=1.122-1.121\left(\frac{a}{w}\right)+3.740\left(\frac{a}{w}\right)^2+3.873\left(\frac{a}{w}\right)^3-19.05\left(\frac{a}{w}\right)^4+22.55\left(\frac{a}{w}\right)^5 \quad (3)$$

for $\frac{a}{w} \le 0.7$

$$F_{II}\left(\frac{a}{w}\right)=\frac{a/w}{\sqrt{\pi(1-a/w)}}\left[7.264-9.37\left(\frac{a}{w}\right)+2.74\left(\frac{a}{w}\right)^2+1.87\left(\frac{a}{w}\right)^3-1.04\left(\frac{a}{w}\right)^4\right] \quad (4)$$

for $0 \le \frac{a}{w} \le 1$

3. RESULTS AND DISCUSSION

3. 1. Microstructur Figure 3 shows the microstructure of the fabricated YSZ /Ni FGM. It has six layers: a pure YSZ layer and five YSZ evidence of agglomerates. As the particle size of the /Ni composite layers containing, 10, 20, 30, 40 and 50 % of Ni content, respectively. The white and gray regions also exhibit the Ni and YSZ phases, respectively. The white area in each composite shows the nickel phase in a grayish ZrO_2 matrix.

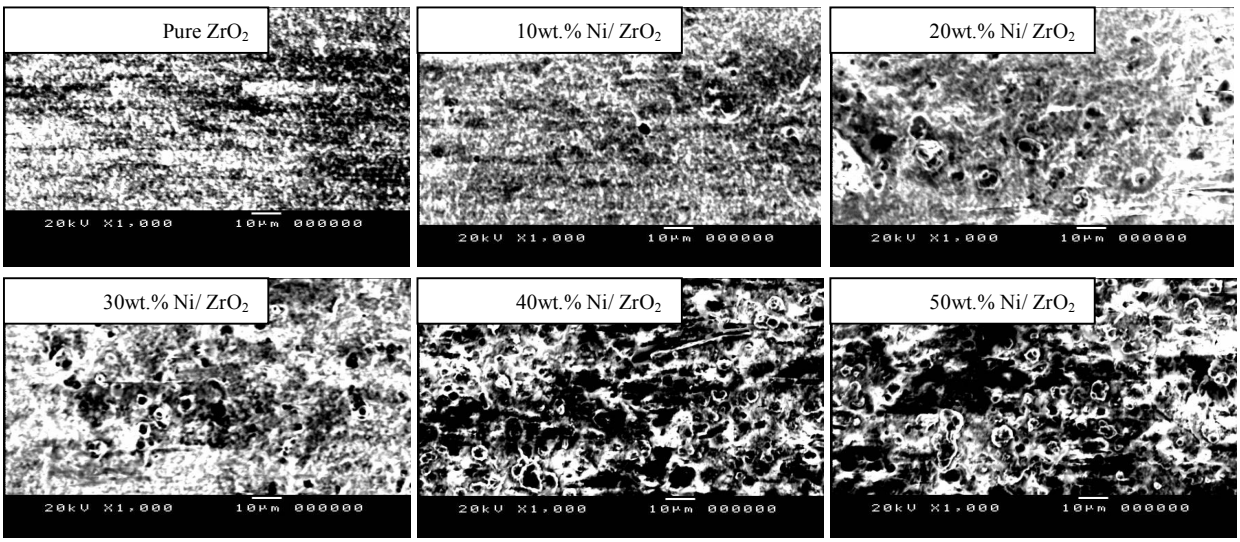

Figure 3. The micrographs of the FGM layers (gray part is nickel in ZrO_2)

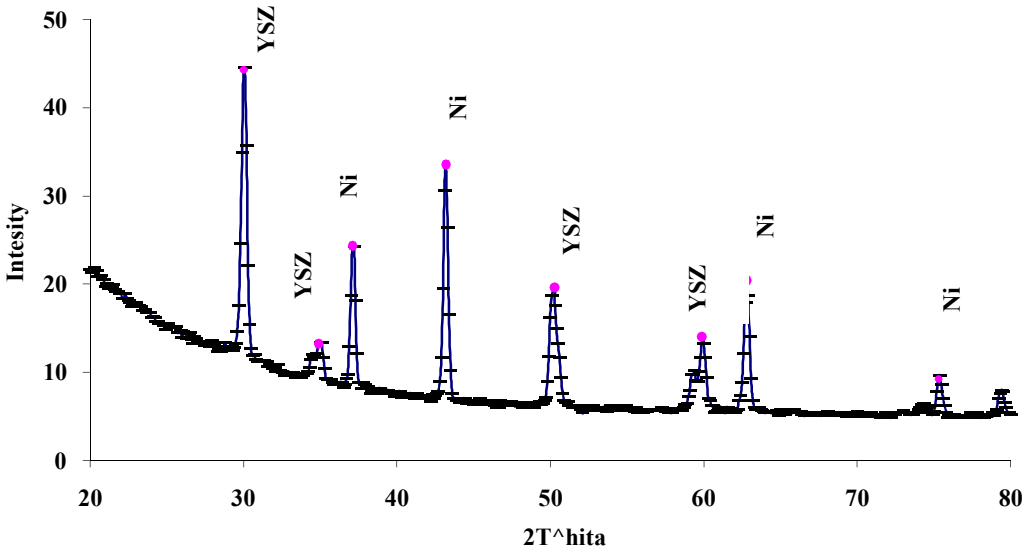

Figure 4. XRD patterns from the surface of the cross-section of the NGCs (YSZ/50%Ni)

3. 2. X-ray Diffraction Patterns The white area increased with increasing Ni contents zirconia powder was considerably smaller than that of the Ni powders, zirconia particles would have entered gaps between Ni particles on the fabrication. As a result, the Ni particles are dispersed in the zirconia matrix in the material with high content of Ni (40%Ni and 50%Ni).

The X-ray diffraction patterns (XRD) from the surface of the cross-section for the NGCs (YSZ /50% Ni) after the presureless sintering under vacuum at 1400 ºC for 2 hour are shown in Figure 4. No new phase was formed between zirconia and Ni during sintering process. No other impurities above the detection limit have been detected. The residual stress (maximum stress) of the NGCs (YSZ/50%Ni) may be determined compared to the pure YSZ at 1700 ºC from the X-ray diffractions using Equation (5).

In the XRD, the maximum strain was measured at the half maximum intensity (I_{max}) of the diffraction angle (2θ) using the line broadening method which are shown in Figure 5(a, b). The residual stress by XRD requires the measurement of the diffractions line shift. If the lines are sharp, it is easily to measure this shift. The breadth (b) was taking at half maximum intensity of the line center for this peak (Equation (6)). It was found that from the Figure 5(a, b), the residual stress (maximum tensile stress) of the non-graded composite (YSZ/50%Ni) was 122 MPa and was in agreement with the published paper.

The residual stress method was estimated from the difference in fracture toughness between the FGM and Non-FGM. In our case, where the composites with high stacking fault energy are heavily deformed, the dislocations entangle to form cell structure causing heterogeneity in the dislocation arrangement. In the dislocation cell structure, the dislocation cell walls are encapsulating the cell interiors in which the dislocation density can be one or two orders of magnitude smaller than in the cell walls.

For our materials which are composed of both soft and ceramic phases, the dislocations generated during the deformation of the soft phase (Ni). The residual stress (maximum stress) of the NGCs (YSZ/50%Ni) may be determined compared to the pure YSZ at 1700 ºC from the X-ray diffractions using Equation (5). In the XRD, the maximum strain was measured at the half maximum intensity (I_{max}) of the diffraction angle (2θ) using the line broadening method which are shown in Figure 5(a, b). The residual stress by XRD requires the measurement of the diffractions line shift. If the lines are sharp, it is easily to measure this shift.

The breadth (b) was taking at half maximum intensity of the line center for this peak (Equation (6)). It was found that from the Figure 5(a, b), the residual stress (maximum tensile stress) of the non-graded composite (YSZ/50%Ni) was 122 MPa and was in agreement with the published paper. The residual stress method was estimated from the difference in fracture toughness between the FGM and Non-FGM. In our case, where the composites with high stacking fault energy are heavily deformed, the dislocations entangle to form cell structure causing heterogeneity in the dislocation arrangement. In the dislocation cell structure, the dislocation cell walls are encapsulating the cell interiors in which the dislocation density can be one or two orders of magnitude smaller than in the cell

walls. For our materials which are composed of both soft and ceramic phases, the dislocations generated during the deformation of the soft phase (Ni) formed loops around the hard zirconia phase and created the dislocation cell structures or the domains. This phenomenon occurred as the generation of dislocations retained the continuity between the two phases to avoid any voids or micro-cracks. Thus, the size of the domains or cells decreased with zirconia contents. The developed techniques for microstructural characterization of deformed polycrystalline materials from asymmetric X-ray line-broadening were studied [17, 18]. Residual stress = E. (Max. Tens. Strain)

$$\text{E.}\left(\frac{1}{2}\right)\left(\frac{\Delta d}{d}\right)=\frac{Eb}{4\tan\theta} \tag{5}$$

$$b=\Delta 2\theta=-2\frac{\Delta d}{d}\tan\theta \tag{6}$$

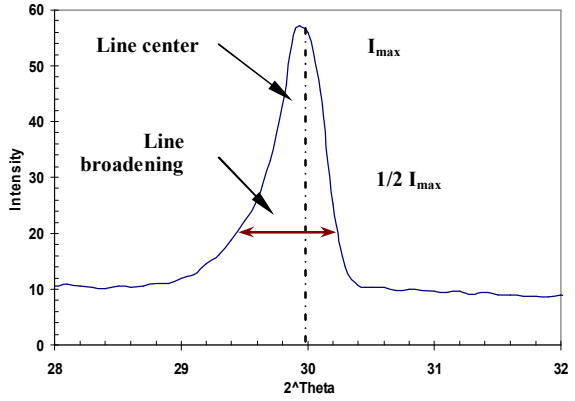

(a)

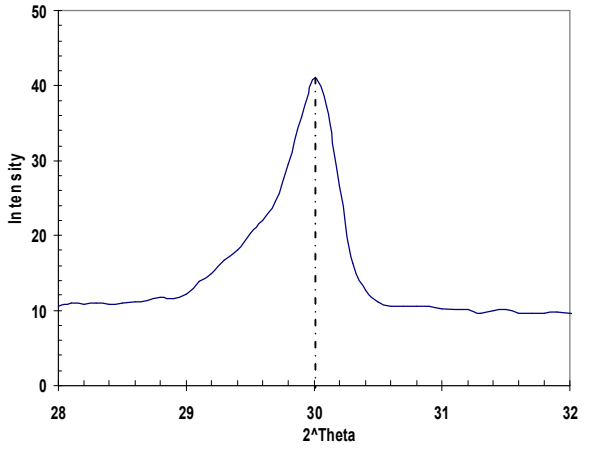

(b)

Figure 5. The line broadening method from XRD for (a) Pure YSZ and (b) NGCs (YSZ/50%Ni)

3. 3. Fracture Toughness According to observation of the specimen side surface during fracture toughness test, a crack was initiated from a notch tip before the maximum load and then the load sharply decreased with crack extension after the maximum load on all NGCs specimens except for 100% YSZ specimen. On the100% YSZ specimen, the stable crack initiation and growth were not observed and unstable fracture from a notch occurred at the maximum load. For pure zirconia, the crack growth occurred intergranuoly at the interfaces under the minimum load. The K_{IC} values are plotted against the material composition of the non-FGM from 0% Ni to 50% Ni in Figure 6. It can be seen, the fracture toughness of the non-graded composite increases almost linearly with an increase in nickel content from0% Ni to 50%Ni. The YSZ has relatively low fracture toughness, with a K_{IC} of about 6 MPa $m^{1/2}$. The K_{IC} of the non-graded composites (non-FGM) is 9.39 MPa $m^{1/2}$ for 10 wt. % Ni, and increases up to 15.72 MPa $m^{1/2}$ for 50 wt. % Ni. This is believed to be the result of the variation of ceramic phase with poor plastic deformation property to the metal phase with good plastic deformation property.

3. 4. Stress Intensity Factors Calculations Table 1 display a comparison between the theoretical results and the finite element modeling for the stress intensity factors (K_I, K_{II}) under the mixed mode loading for the NGC and FGM. The stress intensity factors (K_I and K_{II}) at the crack tip of the three point bending test (3PBT) under mixed mode loading (superposition between the opening mode and shear mode) for the non-graded composite and YSZ /Ni functionally graded materials can be calculated by the Equation (2). The stress intensity factor at the tip of crack depends on geometrical configuration, the loading conditions and material properties of the non-graded composite and YSZ /Ni FGM.

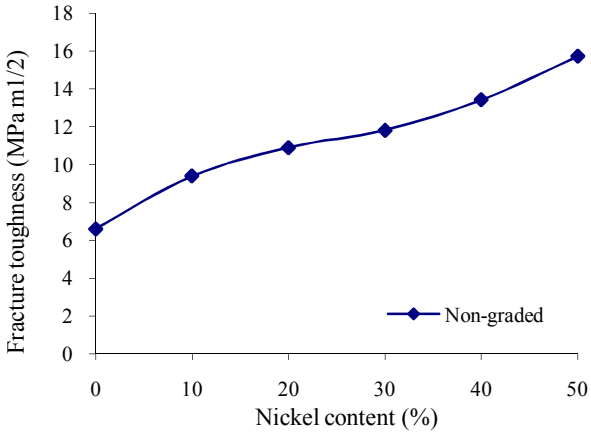

Figure 6. Relation between the fracture toughness and the nickel content

TABLE 1 The SIFs for NGC, FGM-A and FGM-B under mixed mode loading deduced analytically and numerically

Results	NGCs 50%Ni/ZrO_2		FGM-A		FGM-B	
	K_I (MPa$\sqrt{m}$)	K_{II} (MPa$\sqrt{m}$)	K_I (MPa$\sqrt{m}$)	K_{II} (MPa$\sqrt{m}$)	K_I (MPa$\sqrt{m}$)	K_{II} (MPa$\sqrt{m}$)
Analytically from Equations 3.1, 3. 2	12.50	2.42	4.32	1.88	9.67	0.89
Numerically from COSMOS/M 2.70	11.32	1.97	3.77	1.20	8.87	0.66

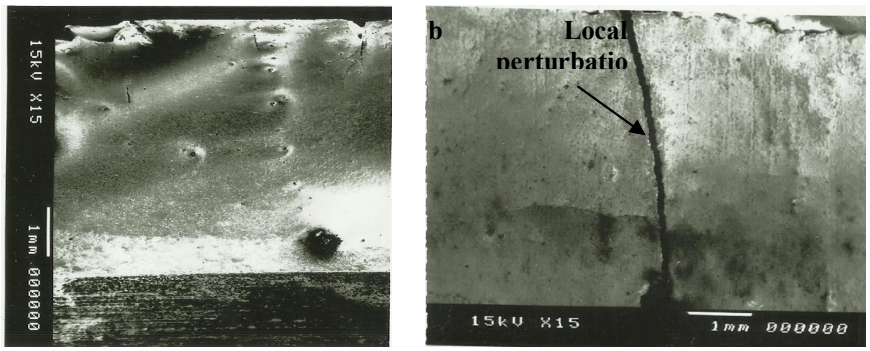

Figure 7. Micrographs of the fractured specimen including: (a) layers of FGM-A (8 layers); (b) FGM-A

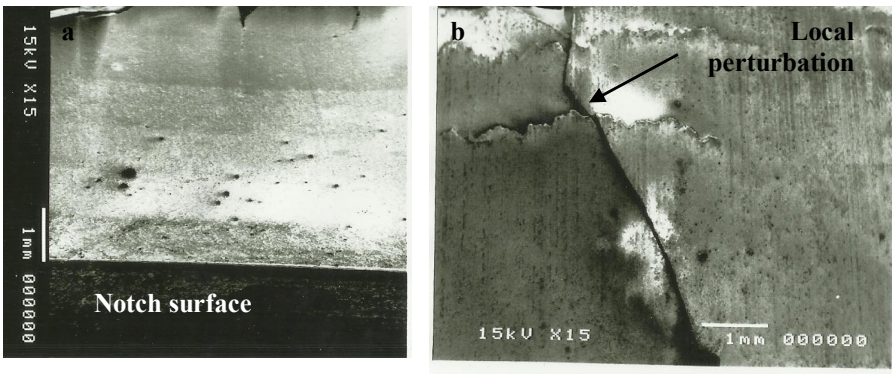

Figure 8. Micrographs of the FGM-B fractured specimen including: (a) 8 layers; (b) crack path& crack propagation angle

FGM-A crack situated in the stiff side of the specimen FGM-B crack situated in the compliant side of the specimen. It can be seen from the table, that the values of K_I , K_{II} for the YSZ /Ni FGM is less than it values NGCs. The Ni particles play an important role in the crack restraint. The Ni particle reduces the SIFs for mode I, mode II near the crack tip. such in the SIFs values for the FGM-A and FGM-B compared to the NGC is attributed to the gradual change in the compositions and properties along the thickness direction of the layers (from phase to another phase). The stress field and stress intensity factor for mode I, mode II were reduced at the crack tip region. In addition, the size of the plastic zone was decreased at the crack tip. The SIFs for the FGM-B was also greater than it values for the FGM-A. This is believed to be to the increasing in nickel content from the stiffness side of specimen. So, once only that the stress intensity factors (K_I, K_{II}) was mainly affected by the elastic gradient (change in elastic modulus) ahead of the crack-tip and the local fracture toughness at the crack-tip.

3. 5. Crack Path and Crack Propagation Angle

The crack path and crack propagation angle were determined according to the maximum principle stress criterion. For this criterion, the crack is propagated in normal direction on the maximum principle stress (MPS). Two types of FGM specimens were analyzed

experimentally: (a) FGM-A corresponds to the specimen with a crack situated on the stiff side of the specimen and propagating along the direction of decreasing elastic modulus, (b) FGM-B corresponds to the specimen with a crack situated on the compliant side of the specimen and propagating along the direction of increasing elastic modulus. The specimen geometry and the experimental conditions were the same for the two FGM specimens. For comparison, a homogeneous specimen with the material composition of 50% Ni/50% YSZ (named by NGC) was also tested under the same experimental conditions. The crack propagation paths of the FGM-A, FGM-B and NGC specimens are shown in Figures 7, 8, 9, respectively. In Figure 7b, the notch-tip of the FGM-A specimen exists in the pure ZrO_2 layer and the crack propagates through the graded region including the layers with 0%, 10%, 20%, 30%, 40% and 50% Ni. In Figure 8b, the notch-tip of the FGM-B specimen locates in the 50% Ni layers and the crack propagates through the graded region including the layers with 50%, 40%, 30%, 20%, 10% and 0% Ni. Figure 9 corresponds to the crack propagation path of the non-graded composite (non-FGM) specimen from these micrographs, the crack propagation paths of the FGM-A, FGM-B and non-graded composite specimens exhibit obvious difference. For FGM-A (Figure 7a), in the region from the pure YSZ layer to the 30% Ni layer, the crack propagates along a straight line at an angle of 9˚ with respect to the orientation of the edge notch. However, in the region of the 40% and 50% Ni layers, the crack curves towards the right edge of the specimen, which is attributed to the effects of the free-edge and the loading-point. Whereas for FGM-B (Figure 8b), in the region from the 50% Ni layer to the 10% Ni layer the crack follows a curved path increases with the crack propagation. The crack in the 10% Ni layer shows an angle of 17 with respect to the orientation of the edge notch. When the crack propagates into the pure YSZ layer, it kinks towards the right edge of the specimen. This is caused by the effects of the free-edge and the loading-point. In addition, the crack in the non-graded composite specimen shows a continuous growth along a straight line except for a little perturbation, as shown in Figure 9. There are some local perturbations in the crack propagation paths of the FGM-A, FGM-B and NGC specimens, respectively, as shown in Figure 6 to Figure 9. Furthermore, most of local perturbations exhibit in the layers with high Ni content such as the layers with 30%, 40% and 50% Ni, respectively. The local perturbations are believed to be caused by the local heterogeneity of the microstructure. The crack trajectory in the layers with 20% and 10% Ni is similar straight without obvious perturbations.

Figure 10 shows the stress distribution around the crack tip with magnified scale of the FGM-A specimen. As shown in chart, the value of the principle stress was high, theoretically tending to infinite (stress singularity) at the crack tip and reduced as the redial distance is increased. It can be see from the stress distributions at the crack tip that the point of the maximum principle stress distribution was tangential to the crack tip.

It is obvious that the crack propagated in the direction normal on the tangential stress and in the path of center of maximum stress contours at the crack tip plastic zone according to maximum principle stress theory. The initial propagation direction was approximately predicted as θ =12 º, as indicated in this figure, in good agreement with the estimated propagation direction of the experimental result as shown in Figure 7a. The crack propagation path of the alumina-epoxy composite and layered were investigated by Tilbrook et al. [19] . Local heterogeneity associated with the interpenetrating composite structure had a perturbing effect on crack path, which averaged out and did not appear to influence the overall propagation path. The comparison between the experimental, theoretical results of the crack propagation angle for non-FGM and FGM-A and FGM-B are listed in Table 2.

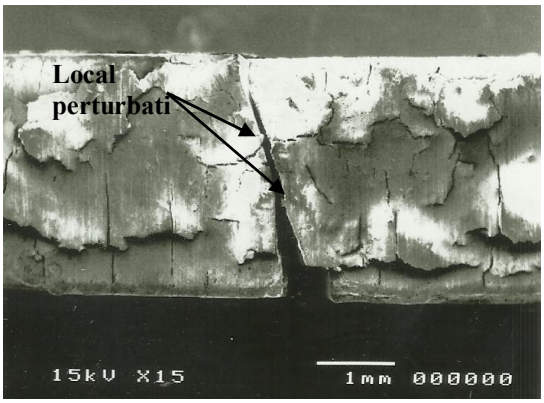

Figure 9. Micrographs of the fractured specimen of the NGC (50%Ni/ YSZ)

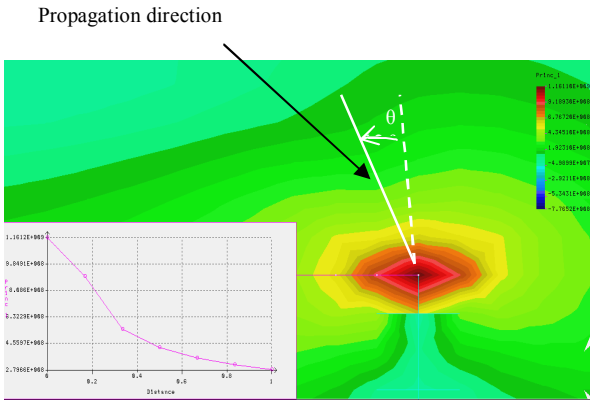

Figure 10. Crack propagation direction for mixed mode of FGM-A, numerically

TABLE 2. Comparison between the Experimental, Theoretical results of the crack propagation angle for NGCs and FGM.

Results	NGC	FGM-A	FGM-B
	α °	α°	α°
Analytically from Equation s 3.12	13	10	15
Experimentally from Figure 6.45a-c	10	9	12
Numerically from Cosmos/M 2.6	11	8	14

4. CONCLUSIONS

1. The fracture toughness obtained by the non- graded composite increases from 6.60 to 15.70 $m^{1/2}$ MPa with an increase in nickel content from 0% to 50% Ni. The fracture toughness for the functionally graded materials was 31.48 MPa $m^{1/2}$.
2. The tensile residual stress of the non-graded composite (YSZ /50%Ni) from XRD line broadening was 122 MPa and was in agreement with the published paper.
3. The values of the stress intensity factors (K_I, K_{II}) for the FGM A and FGM B was less than their corresponding values for pure ceramic (ZrO_2) for the effect of mixed mode loading. Moreover, it was found that the SIFs for the FGM A was greater than those for the FGM B.
4. There are some local perturbations in the crack propagation paths of the FGM-A, FGM-B and non-FGM specimens. Most of local perturbations exhibit in the layers with high Ni content such as the layers with 30, 40 and 50% Ni, respectively. The local perturbations are believed to be caused by the local heterogeneity of the microstructure.
5. The maximum principle stress criterion (MPS) was effective to predict the mixed-mode fracture of FGMs and non-graded specimens.
6. By numerical modeling, the initial propagation direction of the non-graded composites and FGM specimens was approximately predicted as the range (7 - 15 °) according to MPS theory and was in good agreement with the estimated propagation direction of the experimental result.

5. REFERENCES

1. Neubrand, A. and Rödel, J., "Gradient materials: An overview of a novel concept", ***Zeitschrift für Metallkunde***, Vol. 88, No. 5, (1997), 358-371.
2. Amada, S., "Hierarchical functionally gradient structures of bamboo, barley, and corn", ***MRS Bulletin-Materials Research Society***, Vol. 20, No. 1, (1995), 35-36.
3. Hirai, T., Sasaki, M. and Niino, M., "Cvd in situ ceramic composites", ***Journal Society Material Science, Jpn.***, Vol. 36, No. 410, (1987), 1205-1211.
4. Xia, Q. and Wang, M. Y., "Simultaneous optimization of the material properties and the topology of functionally graded structures", ***Computer-Aided Design***, Vol. 40, No. 6, (2008), 660-675.
5. Miyamoto, Y., Kaysser, W., Rabin, B., Kawasaki, A. and Ford, R., "Functionally graded materials: Design, processing and applications", Kluwer, Dordrecht, the Netherlands, Ford R G, (1999).
6. Dolbow, J. and Gosz, M., "On the computation of mixed-mode stress intensity factors in functionally graded materials", ***International Journal of Solids and Structures***, Vol. 39, No. 9, (2002), 2557-2574.
7. Becker Jr, T., Cannon, R. and Ritchie, R., "Finite crack kinking and T-stresses in functionally graded materials", ***International Journal of Solids and Structures***, Vol. 38, No. 32, (2001), 5545-5563.
8. Abanto-Bueno, J. and Lambros, J., "An experimental study of mixed mode crack initiation and growth in functionally graded materials", ***Experimental Mechanics***, Vol. 46, No. 2, (2006), 179-196.
9. Rao, B. and Rahman, S., "Continuum shape sensitivity analysis of a mixed-mode fracture in functionally graded materials", ***Computer Methods in Applied Mechanics and Engineering***, Vol. 194, No. 18, (2005), 1913-1946.
10. Jin, X., Wu, L., Guo, L., Yu, H. and Sun, Y., "Experimental investigation of the mixed-mode crack propagation in ZrO_2/NiCr functionally graded materials", ***Engineering Fracture Mechanics***, Vol. 76, No. 12, (2009), 1800-1810.
11. Jin, X., Wu, L., Sun, Y. and Guo, L., "Microstructure and mechanical properties of ZrO_2/NiCr functionally graded materials", ***Materials Science and Engineering: A***, Vol. 509, No. 1, (2009), 63-68.
12. Kim, J. H. and Paulino, G. H., "Mixed-mode crack propagation in functionally graded materials", in Materials Science Forum, Trans Tech Publ. Vol. 492, (2005), 409-414.
13. Tohgo, K., Iizuka, M., Araki, H. and Shimamura, Y., "Influence of microstructure on fracture toughness distribution in ceramic–metal functionally graded materials", ***Engineering Fracture Mechanics***, Vol. 75, No. 15, (2008), 4529-4541.
14. EL-Wazery, S. M., EL-Desouky, R. A., Hamed A. O., Mansour A. N. and Hassan, A. A., , "Fabrication and mechanical properties of zirconia/nickel functionally graded materials", ***International Journal of Advanced Materials Research***, Vol. 463-464, (2012), 463-471.
15. EL-Wazery, M., EL-Desouky, A., Hamed, O., Fathy, A. and Mansour, N., "Electrical and mechanical performance of zirconia-nickel functionally graded materials", ***International Journal of Engineering-Transactions A: Basics***, Vol. 26, No. 4, (2013), 375.
16. Cannillo, V., Lusvarghi, L., Manfredini, T., Montorsi, M., Siligardi, C., and Sola, A., "Glass–ceramic functionally graded materials produced with different methods", ***Journal of the European Ceramic Society***, Vol. 27, No. 2, (2007), 1293-1298.
17. Mughrabi, H., Ungar, T., Kienle, W. and Wilkens, M., "Long-range internal stresses and asymmetric x-ray line-broadening in tensile-deformed [001]-orientated copper single crystals", ***Philosophical Magazine A***, Vol. 53, No. 6, (1986), 793-813.
18. Sarkar, A., Mukherjee, P. and Barat, P., "X-ray diffraction studies on asymmetrically broadened peaks of heavily deformed zirconium-based alloys", ***Materials Science and Engineering: A***, Vol. 485, No. 1, (2008), 176-181.
19. Tilbrook, M. and Hoffman, M., "Implementation of the local symmetry criterion for crack-growth simulations", in Structural Integrity and Fracture International Conference (SIF'04), (2004), 339-344.

Mixed Mode Crack Propagation of Zirconia/Nickel Functionally Graded Materials

A. R. EL-Desouky, M. S. EL-Wazery

Department of Production Engineering and Mechanical Design, Faculty of Engineering, Menoufiya University, Shebin El-Kom, Egypt

P A P E R I N F O

Paper history:
Received 08 February 2013
Received in revised form 23 May 2013
Accepted 20 June 2013

Keywords:
Functionally Graded Materials (FGM)
Powder Metallurgy Technique
Mixed Mode Fracture
Finite Element Method
Non-graded Composite (NGCS)
Maximum Principle Stress (MPS)

چکیده

مواد عامل دار دانه بندی شده نیکل- زیرکونیوم توسط روش فلزکاری گردی بدست آمده است. میکروساختار، استرس باقیمانده، سفتی ترک و سختی ویکرز مورد بررسی قرار گرفت. پاسخ ترک حالت مرکب مواد عامل دار دانه بندی شده YSZ/Ni با استفاده از آزمایش خمش سه نقطه ای و روش جزء محدود (Cosmos/M 2.7) بررسی شد. نتایج نشان داد که شدت پارامترهای استرس(K_I, K_{II}) برای FGM کمتر از آن چیزی است که برای ترکیبات غیر دانه بندی نشده (NGCs) تحت شرایط بارگذاری حالت مرکب وجود دارد. تعدادی اختلال محلی در مسیرهای انتشار شکست نمونه های FGM و NGC وجود دارد. اغلب اختلال های محلی در لایه هایی با میزان نیکل بالا مانند٪۳۰، ٪۴۰ و ٪۵۰ نشان داده می شوند. این باور وجود دارد که اختلال های محلی توسط غیر همگون بودن میکروساختارها بوجود می آیند. استرس باقیمانده (استرس کششی بیشینه) برای NGC (YSZ/50%Ni) برابر با ۱۲۲ MPa بود که با مقاله های چاپ شده مطابقت داشت.

doi: *10.5829/idosi.ije.2013.26.08b.10*